Available online at http://scik.org
J. Math. Comput. Sci. 2026, 16:3
https://doi.org/10.28919/jmcs/9711
ISSN: 1927-5307

MODELLING YELLOW FEVER CONTROL IN THE PRESENCE OF TOXIC INFECTIONS

MUSAH KONLAN*

Department of Mathematics and Statistics, University of Energy and Natural Resources, Sunyani, Ghana

Abstract. Yellow fever is one of the re-emerging Neglected Tropical Diseases with high socio-economic burden in Africa and Tropical Southern America. In this study, a compartmentalized epidemic model for yellow fever with a toxic infected host population is formulated to explore the dynamics of the disease in a community. The model's disease-free equilibrium state is shown to admit a local and global asymptotic stability whenever the model's reproductive number (R_0) is less than one. Furthermore, using the Descartes Rule of Sign Change, the conditions for the existence of a global asymptotic unique endemic equilibrium have been elaborated. The normalized forward sensitivity index formula is used to determine the relative contributions of the model parameters to the endemicity of yellow fever. These results revealed that yellow fever epidemic is highly sensitive to the removal and biting rates of the disease vectors. Numerical simulations were also performed to investigate the impact of different vaccination and vector biting rates.

Keywords: yellow fever; toxic infections; stability; local sensitivity analysis.

2020 AMS Subject Classification: 92D30.

1. INTRODUCTION

Yellow fever is an acute viral infection transmitted among humans and primates through the bites of an infected female 'Aedes aegypti' mosquito [1, 2]. It is currently one of the Neglected

*Corresponding author

E-mail address: musah.konlan@uenr.edu.gh

Received November 24, 2025

Tropical Diseases with high public and socio-economic impact. Yellow fever is presently endemic in twenty seven and thirteen African and tropical South American countries respectively [3]. Figure 1 indicates the areas in Africa where suspected and confirmed yellow fever disease cases have been recorded from September 2020 to March 2022 [3]. In recent years, the disease has re-emerged and continue to threaten human life. For example, between 2005 and 2016, Sudan experienced three yellow fever outbreaks in which a total of 1508 cases and 368 deaths were recorded [4]. Also, Angola and the Democratic Republic of Congo were hardly hit by the $2015-2016$ yellow fever outbreak which is at the moment classified as the worst ever yellow fever outbreak during the last 37 years [5]. During this outbreak alone, these two countries recorded about 7334 suspected cases of which 962 were confirmed cases and 393 were deaths [6]. Recently, between 2023 and the beginning of 2024, a total of 13 countries in Africa recorded some suspected and confirmed cases of yellow fever (https://www.who.int/emergencies/disease-outbreak-news/item/2024-DON510). According to the Ghana Health Service, in the last quarter of 2021, about 202 suspected cases of yellow fever including 70 confirmed cases and 35 deaths were recorded in the Savannah, Upper West, Bono and Oti regions of the country. Also, in Latin America, Brazil recorded between 1^{st} December 2016 and 8^{th} May 2018, 2050 confirmed cases of yellow fever including 681 deaths with an additional 1300 suspected cases [7]. In 2024, 61 human yellow fever confirmed cases including 30 deaths were recorded in five American countries (see https://www.who.int/emergencies/disease-outbreak-news/item/2024-DON510). Despite the availability of a safe and affordable yellow fever vaccine which has been in use since 1940 [8], the above mentioned outbreaks are clear evidence that yellow fever epidemic still requires attention [9]. Currently, there are no specific antiviral drugs for the treatment of yellow fever. Thus, mass immunization campaigns and vector control are the only reliable means to combat yellow fever epidemics [10]. Mathematical modelling of infectious diseases has been a useful means of providing insight about how diseases outbreaks can be contained and further prevented [11, 12, 13]. Despite the contribution of mathematical modelling in the control of infectious diseases, mathematical modelling works on yellow fever epidemics are very limited. Researchers in [14] formulated and analyzed a yellow fever dynamical model with vertical transmission. Their findings suggested that even though yellow fever vaccination

campaign has positive impact in the community, yellow fever elimination is not feasible with fractional dosing approach. Handari et al. [2] proposed a new yellow fever control model aimed at unveiling how the implementation of control measures such as vaccination, hospitalization and fumigation can reduce yellow fever disease burden in a community. Zhao et al. [5] formulated an epidemic model for the dynamics of infection and control of yellow fever. Their model was used to explore the impact of yellow fever vaccination campaign and the hypothetical delayed vaccination scenario. Authors in [15] constructed a non linear dynamical model to explore the impact of awareness campaigns on yellow fever transmission dynamics. It was established from their study that the rate of awareness campaign and the yellow fever vector removal rate have high potential for reducing the disease endemicity. Fraser et al. [16] proposed a stochastic model to estimate the force of infection and the basic reproductive number for yellow fever epidemics. In reference [10], a mathematical model of yellow fever with toxic infections is presented and analyzed. In most of the few yellow fever models with toxic infections, it is assumed that humans who attained toxic stage do not transmit the disease. However, since not all toxic cases are fatal, we assume in this current study that some humans with toxic infections take part in the disease transmission process.

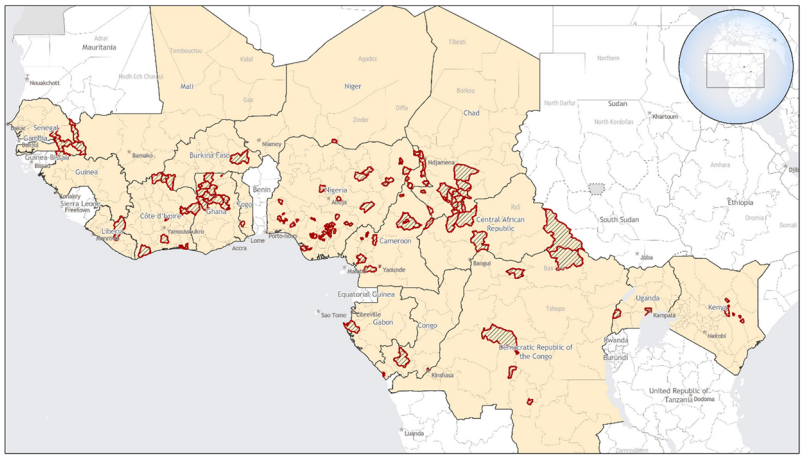

Fig. 1 Yellow fever disease cases — Africa, September 2020-March 2022. Areas with confirmed and probable yellow fever disease cases are outlined in red.

FIGURE 1. Distribution of Yellow Fever in Africa Between September 2020 - March 2022 [3]

2. Development of a Dynamical System for Yellow Fever Transmission

The current expansion of vector-borne diseases to new horizons, coupled with the resurgence of some neglected tropical diseases, calls for the evaluation and recalibration of some existing models to enhance our understanding of the disease transmission process and control. Hence, to construct a mathematical model to investigate the infection dynamics of yellow fever epidemics, we adopt the mathematical models presented in [17, 10] with the assumption that some toxic infected humans contribute to the disease transmission process. This is because it is about $20\% - 50\%$ of the toxic infected people who die between 7 to 10 days [17]. Therefore, it is laudable to assume that some individuals who survive the toxic phase are transmitting the disease. The model consists of hosts (humans) and vectors (female 'Aedes aegypti' mosquitoes) populations. The human sub-population is compartmentalized into five sub-classes (susceptible, (S_h), latently infected/exposed, (E_h), infected, (I_h), toxic infected, (T_h) and recovered, (R_h) individuals). Thus, the sum of all human sub-populations under consideration at time t is: $S_h(t) + E_h(t) + I_h(t) + T_h(t) + R_h(t) = N_h(t)$. The susceptible human population is generated at a rate π_h. Some susceptible humans who are vaccinated at rate ρ attain lifelong protection and move to recovered class. A susceptible who is not vaccinated can become exposed to yellow fever virus through an effective bite from an infected vector at a force of infection λ_h. An exposed human progresses to an infected stage at a rate ϕ. An infected human either recover at rate ω or progress to toxic infected stage at rate σ. Toxic infected people recover at rate γ. The size of each human sub-class is reduced through natural death rate μ_h .

Also, the susceptible vectors are generated at a constant recruitment rate π_v. These susceptible vectors become infected during blood meal from an infected or toxic infected person at a force of infection λ_v. The model assumes constant death rates μ_v for the susceptible and infected vectors. Thus, at any time t, the total mosquito vector population satisfies: $N_v(t) = S_v(t) + I_v(t)$. The forces of infections are given by: $\lambda_h = \frac{b\beta_h I_v}{N_h}$ and $\lambda_v = \frac{b\beta_v(\theta_1 I_h + \theta_2 T_h)}{N_h}$. Figure 2 summarizes the yellow fever model under consideration. Parameters used to construct the model are briefly defined in Table 1.

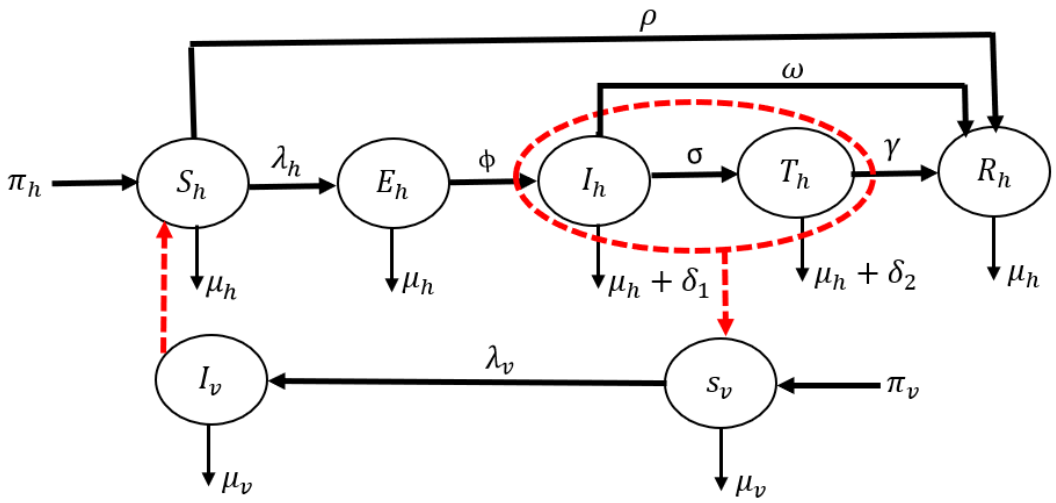

FIGURE 2. Illustrative Diagram for Yellow Fever Transmission Dynamics

$$
\begin{cases}
\dfrac{dS_h}{dt} = \pi_h - \lambda_h S_h - (\rho + \mu_h) S_h \\
\dfrac{dE_h}{dt} = \lambda_h S_h - (\phi + \mu_h) E_h \\
\dfrac{dI_h}{dt} = \phi E_h - (\sigma + \omega + \mu_h + \delta_1) I_h \\
\dfrac{dT_h}{dt} = \sigma I_h - (\gamma + \mu_h + \delta_2) T_h \\
\dfrac{dR_h}{dt} = \omega I_h + \gamma T_h + \rho S_h - \mu_h R_h \\
\frac{dS_v}{dt} = \pi_v - \lambda_v S_v - \mu_v S_v \\
\dfrac{dI_v}{dt} = \lambda_v S_v - \mu_v I_v
\end{cases} \tag{1}
$$

TABLE 1. Yellow Fever Model Variable and Parameter description

Variable	Description	Initial value
$S_h(t)$	Susceptible hosts number at any time t	700
$E_h(t)$	Exposed hosts number at any time t	100
$I_h(t)$	Infected hosts number at any time t	70
$T_h(t)$	Infected toxic hosts number at any time t	0
$R_h(t)$	Recovered hosts number at any time t	10
$S_v(t)$	Susceptible vectors number at any time t	500
$I_v(t)$	Infected vectors number at any time t	30

Parameter	Description	Value[Range]	Reference	Unit
π_h	Human recruitment rate	9.5×10^{-5}	[18]	per day
μ_h	Natural mortality rate of human	4.95×10^{-5}	[10]	per day
β_h	Yellow fever transmission rate from infectious humans to susceptible mosquitoes	0.5	[10]	-
ρ	Effective vaccination rate	[0-0.043]	[5]	per day
ϕ	Rate of progression of exposed humans to infected class	0.31	[10]	per day
σ	Progression rate of humans from infected to toxic stage	0.15	[10]	-
ω	Progression rate from infected humans to recovered class	0.143	[10]	per day
γ	Progression rate of infected humans to recovered class	0.143	[10]	per day
δ_1	Yellow fever induced mortality rate for infected humans	3.5×10^{-4}	[18]	per day
δ_2	Yellow fever induced mortality rate for infected toxic humans	4.0×10^{-4}	Assumed	per day
θ_1	Infectivity level of infected humans	$[0.0 - 1.0]$	Assumed	per day
θ_2	Infectivity level of toxic infected humans	$[0.0 - 1.0]$	Assumed	per day
π_v	Yellow fever mosquito recruitment rate	0.051	[10]	per day
b	Yellow fever mosquito biting rate	$[0.3 - 1.0]$	[5]	per bite
β_v	Disease transmission probability from infected mosquitoes to susceptible humans	0.4	[5]	-
μ_v	Natural death rate of yellow fever vector	0.051	[10]	per day

2.1. Basic Qualitative Properties of the Model Solutions. Under this subsection, we established the well posedness of the model differential equations.

Theorem 1. *The solutions $S_h(t)$, $E_h(t)$, $I_h(t)$, $T_h(t)$, $R_h(t)$, $S_v(t)$, $I_v(t)$ of system (1) are positive and bounded for all time $t \geq 0$ whenever the following initial conditions are satisfied: $S_h(0) \geq 0$, $E_h(0) \geq 0$, $I_h(0) \geq 0$, $T_h(0) \geq 0$, $R_h(0) \geq 0$, $S_v(0) \geq 0$ and $I_v(0) \geq 0$*

Proof. We start by considering the first differential equation of system (1), that is:

$$\frac{dS_h}{dt} = \pi_h - \lambda_h S_h - (\rho + \mu_h) S_h \tag{2}$$

$$\begin{aligned}
&\Longrightarrow \frac{dS_h}{dt} \geq -\lambda_h S_h - (\rho + \mu_h) S_h = -[\lambda_h + (\rho + \mu_h)] S_h \\
&\Longrightarrow \int \frac{dS_h}{S_h} \geq -\int [\lambda_h + (\rho + \mu_h)] dt \\
&\Longrightarrow S_h(t) \geq S_h(0) e^{-[\int_0^t \lambda_h(u)du + (\rho+\mu_h)t]} \geq 0
\end{aligned}$$

Arguing in similar manner, we establish the following:

$$\frac{dE_h}{dt} = \lambda_h S_h - (\phi + \mu_h) E_h \implies E_h(t) \geq E_h(0) e^{-(\phi+\mu_h)t} \geq 0$$

$$\frac{dI_h}{dt} = \phi E_h - (\sigma + \omega + \mu_h + \delta_1) I_h \implies I_h(t) \geq I_h(0) e^{-(\sigma+\omega+\mu_h+\delta_1)t} \geq 0$$

$$\frac{dT_h}{dt} = \sigma I_h - (\gamma + \mu_h + \delta_2) T_h \implies T_h(t) \geq T_h(0) e^{-(\gamma+\mu_h+\delta)t} \geq 0$$

$$\frac{dR_h}{dt} = \omega I_h + \gamma T_h + \rho S_h - \mu_h R_h \implies R_h(t) \geq R_h(0) e^{-\mu_h t} \geq 0$$

$$\frac{dS_v}{dt} = \pi_v - \lambda_v S_v - \mu_v S_v \implies S_v(t) \geq S_v(0) e^{-(\mu_v t + \int_0^t \lambda_v(x)dx)} \geq 0$$

$$\frac{dI_v}{dt} = \lambda_v S_v - \mu_v I_v \implies I_v(t) \geq I_v(0) e^{-\mu_v t} \geq 0$$

Thus, we have established that for $\forall$ t ≥ 0, with non-negative initial state variables values, all solutions of system (1) are non-negative.

Next, we determine the invariant region for system (1).

Theorem 2. *The invariant region for our yellow fever model system of equations is the non-negative set*

$$\Omega = \Omega_{\mathrm{h}} \cup \Omega_{\mathrm{v}} \subset \mathbb{R}_+^5 \times \mathbb{R}_+^2 \tag{3}$$

where

$$\Omega_h = \left\{ (S_h, E_h, I_h, T_h, R_h) \in \mathbb{R}_+^5 : S_h + E_h + I_h + T_h + R_h = N_h \leq \frac{\pi_h}{\mu_h} \right\} \tag{4}$$

and

$$\Omega_v = \left\{ (S_v,\ I_v) \in \mathbb{R}_+^2 :\ S_v + I_v = N_v \leq\ \frac{\pi_v}{\mu_v} \right\} \tag{5}$$

Proof.

Firstly, we determine the subset Ω_{h}.

Summing up the differential equations for the human (host) sub-population from system (1) leads to:

$$\begin{aligned} &\frac{dN_h}{dt} = \pi_h - \mu_h N_h - \delta_1 I_h - \delta_2 T_h \\ \Longrightarrow\ &\frac{dN_h}{dt} \leq \pi_h - \mu_h N_h \ (\text{when} \quad \delta_1 = \delta_2 = 0) \\ \Longrightarrow\ &\frac{dN_h}{N_h - \frac{\pi_h}{\mu_h}} \leq -\mu_h dt \end{aligned} \tag{6}$$

Integrating the last inequality in (6) under the condition that at $t = 0$, $N_h(t) = N_h(0)$, gives: $N_h \leq \frac{\pi_h}{\mu_h}$

Consequently, the following result is obtained

$$0 \leq N_h \leq \frac{\pi_h}{\mu_h} \tag{7}$$

Thus, the subset in (4) is obtained

Secondly, the subset Ω_v is determined. The total female 'Aedes aegypti' mosquito vector population is:

$$N_v = S_v + I_v \tag{8}$$

$$\begin{aligned} \Longrightarrow\ &\frac{d}{dt} N_v = \frac{d}{dt}(S_v + I_v) \\ \Longrightarrow\ &\frac{dN_v}{dt} = \frac{dS_v}{dt} + \frac{dI_v}{dt} \end{aligned}$$

$$\begin{aligned}
&\implies \frac{dN_v}{dt} = \pi_v - \mu_v N_v \\
&\implies N_v - \frac{\pi_v}{\mu_v} = \left(N_v(0) - \frac{\pi_v}{\mu_v}\right) e^{-\mu_v t} as \quad t \to \infty, \quad e^{-\mu_v t} \to 0 \\
&\implies N_v - \frac{\pi_v}{\mu_v} = 0 \quad or \quad N_v = \frac{\pi_v}{\mu_v}.
\end{aligned}$$

Consequently, we have

$$0 \leq N_v \leq \frac{\pi_v}{\mu_v} \tag{9}$$

Therefore, the subsets in (4) and (5) are obtained. Thus, in a nutshell, the dynamical system (1) will be meaningful on the positive set:

$$\Omega = \Omega_h \cup \Omega_v \subset \mathbb{R}_+^5 \times \mathbb{R}_+^2 \tag{10}$$

2.2. Yellow Fever Disease-Free Equilibrium State (YFDFE). It is not hard to see that System (1) possesses a disease-free equilibrium sate denoted by:

$$\xi^* = (S_h^*,\, E_h^*,\, I_h^*,\, T_h^*,\, R_h^*,\, S_v^*,\, I_v^*) = \left(\frac{\pi_h}{\rho + \mu_h},\, 0,\, 0,\, 0,\, \frac{\rho \pi_h}{\mu_h(\rho + \mu_h)},\, \frac{\pi_v}{\mu_v},\, 0\right) \tag{11}$$

2.3. The Basic Reproductive Number ($\mathbf{R}_0$). In epidemiological modelling, R_0 is a significant parameter for assessing the evolution of epidemics. To compute our model's R_0, we express the disease classes of system (1) in the form $\frac{dX_i}{dt} = \mathscr{F}_i(X) - \mathscr{V}_i(X)$, that is, $X = (E_h,\, I_h,\, T_h,\, I_v)$. $\mathscr{F}_i(X)$ and $\mathscr{V}_i(X)$ denote the source of new infection and outflow terms respectively [19]. Thus,

$$\mathscr{F}_i(X) = \begin{pmatrix} \lambda_h S_h \\ 0 \\ 0 \\ \lambda_v S_v \end{pmatrix} \text{ and } \mathscr{V}_i(X) = \begin{pmatrix} (\phi + \mu_h) E_h \\ -\phi E_h + (\sigma + \omega + \mu_h + \delta_1) I_h \\ -\sigma I_h + (\gamma + \mu_h + \delta_2) T_h \\ \mu_v I_v \end{pmatrix} \tag{12}$$

By definition $\mathbf{R_0} = \Lambda(\mathbf{F}\mathbf{V}^{-1})$, where Λ denotes the dominant eigenvalue of $\mathbf{F}\mathbf{V}^{-1}$, $\mathbf{F}$ and $\mathbf{V}$ are the jacobians of $\mathscr{F}_i(X)$ and $\mathscr{V}_i(X)$ evaluated at the DFE point respectively. Now using

$$\frac{\partial \mathscr{F}_i}{\partial X_i} = \begin{pmatrix} \frac{\partial \mathscr{F}_1}{\partial X_1} & \frac{\partial \mathscr{F}_1}{\partial X_2} & \frac{\partial \mathscr{F}_1}{\partial X_3} & \frac{\partial \mathscr{F}_1}{\partial X_4} \\ \frac{\partial \mathscr{F}_2}{\partial X_1} & \frac{\partial \mathscr{F}_2}{\partial X_2} & \frac{\partial \mathscr{F}_2}{\partial X_3} & \frac{\partial \mathscr{F}_2}{\partial X_4} \\ \frac{\partial \mathscr{F}_3}{\partial X_1} & \frac{\partial \mathscr{F}_3}{\partial X_2} & \frac{\partial \mathscr{F}_3}{\partial X_3} & \frac{\partial \mathscr{F}_3}{\partial X_4} \\ \frac{\partial \mathscr{F}_4}{\partial X_1} & \frac{\partial \mathscr{F}_4}{\partial X_2} & \frac{\partial \mathscr{F}_4}{\partial X_3} & \frac{\partial \mathscr{F}_4}{\partial X_4} \end{pmatrix} \text{ and } \frac{\partial \mathscr{V}_i}{\partial X_i} = \begin{pmatrix} \frac{\partial \mathscr{V}_1}{\partial X_1} & \frac{\partial \mathscr{V}_1}{\partial X_2} & \frac{\partial \mathscr{V}_1}{\partial X_3} & \frac{\partial \mathscr{V}_1}{\partial X_4} \\ \frac{\partial \mathscr{V}_2}{\partial X_1} & \frac{\partial \mathscr{V}_2}{\partial X_2} & \frac{\partial \mathscr{V}_2}{\partial X_3} & \frac{\partial \mathscr{V}_2}{\partial X_4} \\ \frac{\partial \mathscr{V}_3}{\partial X_1} & \frac{\partial \mathscr{V}_3}{\partial X_2} & \frac{\partial \mathscr{V}_3}{\partial X_3} & \frac{\partial \mathscr{V}_3}{\partial X_4} \\ \frac{\partial \mathscr{V}_4}{\partial X_1} & \frac{\partial \mathscr{V}_4}{\partial X_2} & \frac{\partial \mathscr{V}_4}{\partial X_3} & \frac{\partial \mathscr{V}_4}{\partial X_4} \end{pmatrix} \tag{13}$$

Evaluating (13) at ξ^* gives

(14)
$$\mathbf{F}=\begin{pmatrix} 0 & 0 & 0 & \frac{b\beta_h\mu_h}{\rho+\mu_h} \\ 0 & 0 & 0 & 0 \\ 0 & 0 & 0 & 0 \\ 0 & \frac{b\beta_v\theta_1\pi_v\mu_h}{\pi_h\mu_v} & \frac{b\beta_v\theta_2\pi_v\mu_h}{\pi_h\mu_v} & 0 \end{pmatrix} \quad \text{and} \quad \mathbf{V}=\begin{pmatrix} \phi+\mu_h & 0 & 0 & 0 \\ -\phi & \sigma+\omega+\mu_h+\delta_1 & 0 & 0 \\ 0 & -\sigma & \gamma+\mu_h+\delta_2 & 0 \\ 0 & 0 & 0 & \mu_v \end{pmatrix}$$

From $\mathbf{V}$, we have:

(15)
$$\mathbf{V^{-1}}=\begin{pmatrix} \frac{1}{\phi+\mu_h} & 0 & 0 & 0 \\ \frac{\phi}{(\phi+\mu_h)(\sigma+\omega+\mu_h+\delta_1)} & \frac{1}{(\sigma+\omega+\mu_h+\delta_1)} & 0 & 0 \\ \frac{\phi\sigma}{(\phi+\mu_h)(\sigma+\omega+\mu_h+\delta_1)(\gamma+\mu_h+\delta_2)} & \frac{\sigma}{(\sigma+\omega+\mu_h+\delta_1)(\gamma+\mu_h+\delta_2)} & \frac{1}{(\gamma+\mu_h+\delta_2)} & 0 \\ 0 & 0 & 0 & \frac{1}{\mu_v} \end{pmatrix}$$

Hence, computing FV^{-1} gives:

(16)
$$FV^{-1}=\begin{pmatrix} 0 & 0 & 0 & \frac{b\beta_h\mu_h}{\mu_v(\rho+\mu_h)} \\ 0 & 0 & 0 & 0 \\ 0 & 0 & 0 & 0 \\ \frac{b\phi\beta_v\pi_v\mu_h[\theta_1(\gamma+\mu_h+\delta_2)+\sigma\theta_2]}{\pi_h\mu_v(\phi+\mu_h)(\sigma+\omega+\mu_h+\delta_1)(\gamma+\mu_h+\delta_2)} & \frac{b\beta_v\pi_v\mu_h[\theta_1(\gamma+\mu_h+\delta_2)+\sigma\theta_2]}{\pi_h\mu_v(\sigma+\omega+\mu_h+\delta_1)(\gamma+\mu_h+\delta_2)} & \frac{b\beta_v\pi_v\mu_h\theta_2}{\pi_h\mu_v(\gamma+\mu_h+\delta_2)} & 0 \end{pmatrix}$$

Computing the eigenvalues of the matrix FV^{-1} gives the largest one as:

(17)
$$\lambda_{max}=\sqrt{\frac{b^2\beta_h\beta_v\phi\pi_v\mu_h^2[\theta_1(\gamma+\mu_h+\delta_2)+\sigma\theta_2]}{\pi_h\mu_v^2(\rho+\mu_h)(\phi+\mu_h)(\sigma+\omega+\mu_h+\delta_1)(\gamma+\mu_h+\delta_2)}}$$

Therefore, the reproductive number of the model is given by:

(18)
$$\begin{aligned} R_0 &= \sqrt{\frac{b^2\phi\beta_h\beta_v\mu_h^2\pi_v[\theta_1(\gamma+\mu_h+\delta_2)+\sigma\theta_2]}{\pi_h\mu_v^2(\phi+\mu_h)(\rho+\mu_h)(\sigma+\omega+\mu_h+\delta_1)(\gamma+\mu_h+\delta_2)}} \\ &= \sqrt{R_{0h}\times R_{0v}} \end{aligned}$$

where:

$$R_{0h}=\frac{b\phi\beta_h\mu_h^2[\theta_1(\gamma+\mu_h+\delta_2)+\sigma\theta_2]}{\pi_h(\phi+\mu_h)(\rho+\mu_h)(\sigma+\omega+\mu_h+\delta_1)(\gamma+\mu_h+\delta_2)} \quad \text{and} \quad R_{0v}=\frac{b\beta_v\pi_v}{\mu_v^2}$$

2.4. Stability of Yellow Fever Disease-Free Equilibrium (YFDFE).

2.4.1. *Local Stability of YFDFE.*

Theorem 3. *The YFDFE* $(\xi^*) = \left(\frac{\pi_h}{\rho+\mu_h},\ 0,\ 0,\ 0,\ \frac{\rho\pi_h}{\mu_h(\rho+\mu_h)},\ \frac{\pi_v}{\mu_v},\ 0\right)$ *admits a local asymptotic stability if* $R_0 < 1$ *and unstable whenever* $R_0 > 1$

Proof. Linearizing system (1) around the YFDFE gives the following matrix denoted by:

$$J(\xi^*) = \begin{pmatrix} -(\rho+\mu_h) & 0 & 0 & 0 & 0 & 0 & -\frac{b\beta_h\mu_h}{(\rho+\mu_h)} \\ 0 & -(\phi+\mu_h) & 0 & 0 & 0 & 0 & \frac{b\beta_h\mu_h}{(\rho+\mu_h)} \\ 0 & \phi & -(\sigma+\omega+\mu_h+\delta_1) & 0 & 0 & 0 & 0 \\ 0 & 0 & \sigma & -(\gamma+\mu_h+\delta_2) & 0 & 0 & 0 \\ \rho & 0 & \omega & \gamma & -\mu_h & 0 & 0 \\ 0 & 0 & -\frac{b\beta_v\theta_1\pi_v\mu_h}{\pi_h\mu_v} & -\frac{b\beta_v\theta_2\pi_v\mu_h}{\pi_h\mu_v} & 0 & -\mu_v & 0 \\ 0 & 0 & \frac{b\beta_v\theta_1\pi_v\mu_h}{\pi_h\mu_v} & \frac{b\beta_v\theta_2\pi_v\mu_h}{\pi_h\mu_v} & 0 & 0 & -\mu_v \end{pmatrix} \tag{19}$$

By observation, the matrix in (19) possesses three negative eigenvalues, namely $\lambda_1 = -(\rho + \mu_h)$ $\lambda_5 = -\mu_h$ and $\lambda_6 = -\mu_v$. Using matrix algebra, the matrix in (19) then reduces to the sub-matrix in (20) below:

$$J_1 = \begin{pmatrix} -(\phi+\mu_h) & 0 & 0 & \frac{b\beta_h\mu_h}{(\rho+\mu_h)} \\ \phi & -(\sigma+\omega+\mu_h+\delta_1) & 0 & 0 \\ 0 & \sigma & -(\gamma+\mu_h+\delta_2) & 0 \\ 0 & \frac{b\beta_v\theta_1\pi_v\mu_h}{\pi_h\mu_v} & \frac{b\beta_v\theta_2\pi_v\mu_h}{\pi_h\mu_v} & -\mu_v \end{pmatrix} \tag{20}$$

$$\text{Now,} \quad Trace(J_1) = -(\phi+\sigma+\omega+\gamma+\delta_1+\delta_2+3\mu_h+\mu_v) < 0 \tag{21}$$

Also, the determinant of (J_1) is

$$\det(J_1) = \mu_v(\phi+\mu_h)(\sigma+\omega+\gamma+\mu_h+\delta_1)(\gamma+\mu_h+\delta_2)\left(1-R_0^2\right) \tag{22}$$

It is clear from (21) and (22) that $Trace(J_1) < 0$ and $\det(J_1) > 0$ if $R_0 < 1$. Thus, matrix J_1 possesses real and negative eigenvalues [20, 21]. Consequently, matrix $J(\xi^*)$ admits eigenvalues with negative real parts. Hence, we conclude that the YFDFE state of system (1) admits a local asymptotic stability whenever $R_0 < 1$ and is unstable otherwise.

2.4.2. *Global Stability of the YFDFE.* Adopting the global stability analysis procedure presented in [11, 12, 13, 22], we investigate the longtime stability status of the YFDFE of system (1). Thus, we first express system (1) in a triangular form as follows:

$$\begin{cases} \frac{dY_s}{dt} = G(Y_s - Y_{sYFDFE}) + KY_i \\ \frac{dY_i}{dt} = LY_i \end{cases} \tag{23}$$

In (23) Y_s and Y_i denote the non-infected/infectious and infected/infectious compartments respectively, that is: $Y_{sYFDFE} = \left(S_h^*, R_h^*, S_v^*\right) = \left(\frac{\pi_h}{\rho+\mu_h}, \frac{\rho\pi_h}{\mu_h(\rho+\mu_h)}, \frac{\pi_v}{\mu_v}\right)$

$$(Y_s - Y_{sYFDFE}) = \begin{cases} S_h - \frac{\pi_h}{\rho+\mu_h} \\ R_h - \frac{\rho\pi_h}{\mu_h(\rho+\mu_h)} \\ S_v - \frac{\pi_v}{\mu_v} \end{cases} \tag{24}$$

$$\begin{cases} G = \frac{\partial Y_s}{\partial(S_h,\, R_h,\, S_v)} \\ K = \frac{\partial Y_s}{\partial(E_h,\, I_h,\, T_h,\, I_v)} \\ L = \frac{\partial Y_i}{\partial(E_h,\, I_h,\, T_h,\, I_v)} \end{cases} \tag{25}$$

Now, evaluating the matrices of partial derivatives in (25) at Y_{sYFDFE}, we get:

$$G = \begin{pmatrix} -(\rho+\mu_h) & 0 & 0 \\ \rho & -\mu_h & 0 \\ 0 & 0 & -\mu_v \end{pmatrix} \tag{26}$$

$$K = \begin{pmatrix} 0 & 0 & 0 & -\frac{b\beta_h\mu_h}{(\rho+\mu_h)} \\ 0 & \omega & \gamma & 0 \\ 0 & -\frac{b\beta_v\theta_1\mu_h\pi_v}{\pi_h\mu_v} & -\frac{b\beta_v\theta_2\mu_h\pi_v}{\pi_h\mu_v} & 0 \end{pmatrix} \tag{27}$$

$$L = \begin{pmatrix} -(\phi+\mu_h) & 0 & 0 & \frac{b\beta_h\mu_h}{(\rho+\mu_h)} \\ \phi & -(\sigma+\omega+\mu_h+\delta_1) & 0 & 0 \\ 0 & \sigma & -(\gamma+\mu_h+\delta_2) & 0 \\ 0 & \frac{b\beta_v\theta_1\mu_h\pi_v}{\pi_h\mu_v} & \frac{b\beta_v\theta_2\mu_h\pi_v}{\pi_h\mu_v} & -\mu_v \end{pmatrix} \tag{28}$$

Using the above matrices, we state the following theorem.

Theorem 4. *The system* $\frac{dY_s}{dt} = G(Y_s - Y_{sYFDFE}) + KY_i$ *admits a global asymptotic stability at the YFDFE if G is a matrix of real negative eigenvalues and L is a stable Metzler matrix.*

By simple observation, see that matrix G admits only negative real eigenvalues. Additionally, matrix L is clearly a Metzler type. Next, we use the following theorem from [23, 24] to test for its stability.

Theorem 5. *If* $\mathscr{L}$ *is a Metzler matrix that can be partitioned in blocks as*

$$\mathscr{L} = \begin{pmatrix} L_1 & L_2 \\ L_3 & L_4 \end{pmatrix}, \tag{29}$$

with L_1 *and* L_4 *being square matrices, then the stability of matrix* $\mathscr{L}$ *is guaranteed if and only if the matrix* $L_1 - L_2L_4^{-1}L_3$ *is Metzler stable*

Now using (28) it is not hard to see that matrix L can be partitioned in the form of (29) with

$$L_1 = \begin{pmatrix} -(\phi+\mu_h) & 0 \\ \\ \phi & -(\sigma+\omega+\mu_h+\delta_1) \end{pmatrix} \qquad L_2 = \begin{pmatrix} 0 & \frac{b\beta_h\mu_h}{(\rho+\mu_h)} \\ \\ 0 & 0 \end{pmatrix}$$

(30)

$$L_3 = \begin{pmatrix} 0 & \sigma \\ \\ 0 & \frac{b\beta_v\theta_1\mu_h\pi_v}{\pi_h\mu_v} \end{pmatrix} \qquad L_4 = \begin{pmatrix} -(\gamma+\mu_h+\delta_2) & 0 \\ \\ \frac{b\beta_v\theta_2\mu_h\pi_v}{\pi_h\mu_v} & -\mu_v \end{pmatrix}$$

From (30), we have

$$L_1 - L_2L_4^{-1}L_3 = \begin{pmatrix} -(\phi+\mu_h) & \frac{b^2\beta_h\beta_v\mu_h^2\pi_v[\theta_1(\gamma+\mu_h+\delta_2)+\sigma\theta_2]}{\pi_h\mu_v^2(\rho+\mu_h)(\gamma+\mu_h+\delta_2)} \\ \\ \phi & -(\sigma+\omega+\mu_h+\delta_1) \end{pmatrix}, \tag{31}$$

Now matrix $L_1 - L_2L_4^{-1}L_3$ is stable if it has a negative trace and strictly positive determinant [20]. It is easy to see that $trace(L_1 - L_2L_4^{-1}L_3) = -(\phi+\mu_h)(\sigma+\omega+\mu_h+\delta_1) < 0$. Also, $\det(L_1 - L_2L_4^{-1}L_3) = (\phi+\mu_h)(\sigma+\omega+\mu_h+\delta_1)\left(1-R_0^2\right) > 0$ if and only if $R_0 < 1$

Thus, we conclude that the global asymptotic stability of system

$$\frac{dY_s}{dt} = G\left(Y_s - Y_{sYFDFE}\right) + KY_i \tag{32}$$

is guaranteed only if $R_0 < 1$.

2.5. Yellow Fever Endemic Equilibrium Point/State (YFEEP). The YFEEP is the non-trivial solution of the system (1) at the point when yellow fever disease persists in the community. If, we denote the YFEEP by $\xi^{**} = (S_h^{**},\ E_h^{**},\ I_h^{**},\ T_h^{**},\ R_h^{**},\ S_v^{**},\ I_v^{**})$ then ξ^{**} satisfies the system:

$$
\begin{cases}
\pi_h - \lambda_h^{**} S_h^{**} - (\rho + \mu_h) S_h^{**} = 0 \\
\lambda_h^{**} S_h^{**} - (\phi + \mu_h) E_h^{**} = 0 \\
\phi E_h^{**} - (\sigma + \omega + \mu_h + \delta_1) I_h^{**} = 0 \\
\sigma I_h^{**} - (\gamma + \mu_h + \delta_2) T_h^{**} = 0 \\
\rho S_h^{**} + \gamma T_h^{**} + \omega I_h^{**} - \mu_h R_h^{**} = 0 \\
\pi_v - \lambda_v^{**} S_v^{**} - \mu_v S_v^{**} = 0 \\
\lambda_v^{**} S_v^{**} - \mu_v I_v^{**} = 0
\end{cases} \tag{33}
$$

Thus, solving for S_h^{**}, E_h^{**}, I_h^{**}, T_h^{**}, R_h^{**}, S_v^{**} and I_v^{**} in (33) leads to the following system:

$$
\begin{cases}
S_h^{**} = \frac{\pi_h^2 \mu_v \left(\pi_h \mu_v (\gamma+\mu_h+\delta_2) + b\beta_v \mu_v [(\gamma+\mu_h+\delta_2)\theta_1 + \sigma\theta_2] I_h^{**}\right)}{(\rho+\mu_h)(\gamma+\mu_h+\delta_2)(\pi_h\mu_v)^2 + b\beta_v\mu_h[\theta_1(\gamma+\mu_h+\delta_2)+\sigma\theta_2][b\beta_h\pi_v\mu_h + \pi_h\mu_v(\rho+\mu_h)]I_h^{**}} \\
E_h^{**} = \frac{b^2\beta_h\beta_v\pi_v\mu_h^2(\theta_1(\gamma+\mu_h+\delta_2)+\sigma\theta_2)I_h^{**}}{(\gamma+\mu_h+\delta_2)(\pi_h\mu_v)^2 + b\beta_v\pi_h\mu_h\mu_v(\theta_1(\gamma+\mu_h+\delta_2)+\sigma\theta_2)(\phi+\mu_h)I_h^{**}} S_h^{**} \\
T_h^{**} = \frac{\sigma}{(\gamma+\mu_h+\delta_2)} I_h^{**} \\
R_h^{**} = \frac{1}{\mu_h(\gamma+\mu_h+\delta_2)} \left[\rho(\gamma+\mu_h+\delta_2)S_h^{**} + (\sigma\gamma + \omega(\gamma+\mu_h+\delta_2))I_h^{**}\right] \\
S_v^{**} = \frac{\pi_h\pi_v(\gamma+\mu_h+\delta_2)}{\pi_h\mu_v(\gamma+\mu_h+\delta_2) + b\beta_v\mu_h[\theta_1(\gamma+\mu_h+\delta_2)+\sigma\theta_2]I_h^{**}} \\
I_v^{**} = \frac{b\beta_v\mu_h\pi_v[\theta_1(\gamma+\mu_h+\delta_2)+\sigma\theta_2]I_h^{**}}{(\gamma+\mu_h+\delta_2)\pi_h\mu_v^2 + b\beta_v\mu_h\mu_v[\theta_1(\gamma+\mu_h+\delta_2)+\sigma\theta_2]I_h^{**}} \\
\text{where } I_h^{**} \text{ satisfies} \quad \kappa_2 I_h^{**2} + \kappa_1 I_h^{**} + \kappa_0 = 0
\end{cases} \tag{34}
$$

With:

$$
\begin{cases}
\kappa_2 = b^2\beta_h\beta_v\mu_h^2\left((\gamma+\mu_h+\delta_2)\theta_1 + \sigma\theta_2\right)^2\left(b\beta_h\pi_v\mu_h + \pi_h\mu_v\right) \\
\kappa_1 = b\beta_v\pi_h^2\mu_h\mu_v(\gamma+\mu_h+\delta_2)\left(\sigma\theta_2 + \theta_1(\gamma+\mu_h+\delta_2)\right)\left[b\beta_h\pi_v\mu_h + \pi_h\mu_v(\rho+\mu_h)(2-{R_0}^2)\right] \\
\kappa_0 = \pi_h^4\mu_v^3(\rho+\mu_h)(\gamma+\mu_h+\delta_2)(1-{R_0}^2)
\end{cases} \tag{35}
$$

To discuss the uniqueness of the YFEEP, we use the Descartes Rule of Sign Change to obtain table 2 below.

TABLE 2. Possible Number (#) of YFEEP

Case	κ_2	κ_1	κ_0	R_0	# of Sign Change	# of Roots
(i)	+	+	−	$R_0 > 1$	1	1
(ii)	+	−	−	$R_0 > 1$	1	1
(iii)	+	+	+	$R_0 < 1$	0	0

Using Table 2, we elaborate the following results:

Theorem 6. *At the disease persistence state, system (1) admits:*
(i) only one YFEEP if $R_0 > 1$.
(ii) no YFEEP if $R_0 < 1$

Thus, in the next section, we use a Lyapunov function to explore the stability status of this YEEEP within its global neighborhood.

2.5.1. *Global Stability of YFEEP.*

Theorem 7. *The unique YFEEP* (ξ^{**}) *of system (1) admits a global asymptotic stability whenever it exists (*$R_0 > 1$*).*

Proof. As in Konlan et al. [11], we consider a positive definite function $\mathscr{H}$ defined by:

$$\mathscr{H}(x) = \sum_{i=1}^{n} \frac{1}{2}(x_i - x_i^{**})^2 \quad i = i^{th}\text{model compartment}$$

Now,

$$\begin{aligned} \mathscr{H}(\xi^{**}) = &\frac{1}{2}\left(S_h - S_h^{**} + E_h - E_h^{**} + I_h - I_h^{**} + T_h - T_h^{**} + R_h - R_h^{**}\right)^2 \\ &+ \frac{1}{2}\left(S_v - S_v^{**} + I_v - I_v^{**}\right)^2 \end{aligned} \tag{36}$$

Taking the time derivative of $\mathscr{H}$ gives

$$\begin{aligned}\frac{d}{dt}\mathscr{H}(\xi^{**}) &= (S_h - S_h^{**} + E_h - E_h^{**} + I_h - I_h^{**} + T_h - T_h^{**} + R_h - R_h^{**}) \\ &\quad \left[\frac{d}{dt}(S_h + E_h + I_h + T_h + R_h)\right] + (S_v - S_v^{**} + I_v - I_v^{**})\frac{d}{dt}(S_v + I_v) \\ &= (S_h - S_h^{**} + E_h - E_h^{**} + I_h - I_h^{**} + T_h - T_h^{**} + R_h - R_h^{**})\frac{dN_h}{dt} \\ &\quad + (S_v - S_v^{**} + I_v - I_v^{**})\frac{dN_v}{dt}\end{aligned} \tag{37}$$

Using $\frac{dN_h}{dt} = \pi_h - \mu_h N_h - \delta_1 I_h - \delta_2 T_h$ and $\frac{dN_v}{dt} = \pi_v - \mu_v N_v$, we obtain

$$\begin{aligned}\frac{d}{dt}\mathscr{H}(\xi^{**}) &= (N_h - N_h^{**})(\pi_h - \mu_h N_h - \delta_1 I_h - \delta_2 T_h) + (N_v - N_v^{**})(\pi_v - \mu_v N_v) \\ &\leq (N_h - N_h^{**})(\pi_h - \mu_h N_h) + (N_v - N_v^{**})(\pi_v - \mu_v N_v) \\ &\leq (N_h - N_h^{**})\left[-\mu_h\left(N_h - \frac{\pi_h}{\mu_h}\right)\right] + (N_v - N_v^{**})\left[-\mu_v\left(N_v - \frac{\pi_v}{\mu_v}\right)\right]\end{aligned} \tag{38}$$

At the endemic point, we have $N_h^{**} = \frac{\pi_h}{\mu_h}$ and $N_v^{**} = \frac{\pi_v}{\mu_v}$, this implies

$$\frac{d}{dt}\mathscr{H}(\xi^{**}) \leq -\mu_h (N_h - N_h^{**})^2 - \mu_v (N_v - N_v^{**})^2 \leq 0 \tag{39}$$

□

Clearly, $\frac{d\mathscr{H}(\xi^{**})}{dt} \leq 0$ with equality holding if and only if $N_h^{**} = N_h$ and $N_v^{**} = N_v$, thus, according to [11, 25, 26], (ξ^{**}) (yellow fever endemic equilibrium state) admits a global asymptotic stability whenever it exists.

3. Sensitivity Analysis

In order to optimize resources, disease control experts normally advocate for the implementation of control measures targeting the most influential parameters in any disease outbreak. Hence, the usefulness of sensitivity analysis to identify these parameters. The sensitivity index of a parameter say, k of the threshold quantity R_0 is defined using partial derivative as:

$$\Gamma_k^{R_0} = \frac{k}{R_0} \times \frac{\partial R_0}{\partial k} \tag{40}$$

Using the relation in (40) and table (3), we obtained for example:

$$\Gamma_\rho^{R_0} == \frac{-\rho}{2(\rho + \mu_h)} = -0.4975372, \quad \Gamma_\phi^{R_0} = \frac{\mu_h}{2(\phi + \mu_h)} = +7.9825963 \times 10^{-5}$$

Similarly, we tabulate the results as shown below.

TABLE 3. Sensitivity Indices for R_0 Parameters

Parameter	**Index**
π_h	-0.50
b	$+1.00$
β_h	$+0.50$
μ_h	$+0.4973318$
ρ	-0.4975372
ϕ	$+7.9825963 \times 10^{-5}$
ω	-0.2436950
σ	-0.1362288
γ	-0.1190213
θ_1	$+0.3806046$
θ_2	$+0.1193954$
δ_1	$-5.9645637 \times 10^{-4}$
δ_2	$-3.3292659 \times 10^{-4}$
π_v	$+0.50$
β_v	$+0.50$
μ_v	-1.00

The results in Table 3 above indicate that parameters $b,\ \beta_h,\ \beta_v, \phi,\ \pi_v,\ \theta_1$ and θ_2 have positive indices. This means that a decrease in any of these parameter values while keeping all other model parameters constant will result in a reduction in the endemicity of yellow fever epidemics. In contrast, the parameters $\mu_v,\ \rho, \omega$ and γ have negative indices. Thus, an increase in any of these parameter values when all other model parameters remain constant will lead to a decrease in the persistence of yellow fever in the community. Hence, our results suggest that prioritizing control measures aimed at increasing the removal rate or minimizing the biting rate of yellow fever disease vectors may help mitigate the disease in its endemic regions.

4. NUMERICAL SIMULATIONS

In order to substantiate our theoretical findings, we carried out numerical simulations using Matlab ode45 solver. This was performed using the values from Table 1. The graphical solutions are presented below (Figure 3 to Figure 12). Figure 3 gives the evolution of all the population sub-classes. Figures 4 to 10 demonstrate the impact of varying effective vaccination rate on the model population sub-classes. Finally, Figures 11 to 14 demonstrate the effect of different yellow fever vector effective biting rate on the model disease sub-classes. It can be observed from Figure 4 that increasing the effectiveness of yellow fever vaccination reduces the susceptible population.

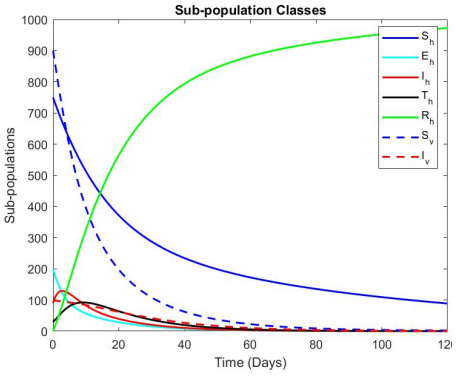

FIGURE 3. Population Classes

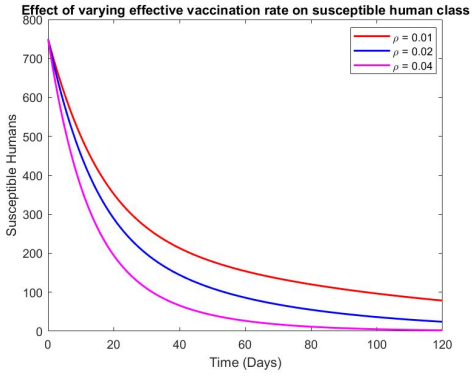

FIGURE 4. Susceptible Humans

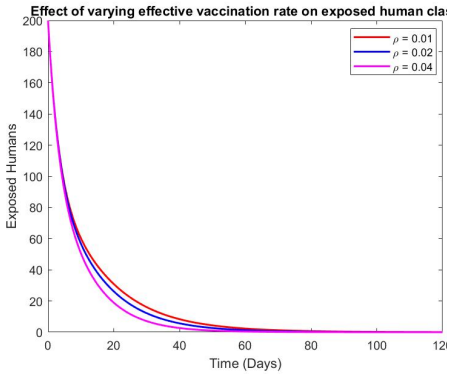

FIGURE 5. Exposed Humans

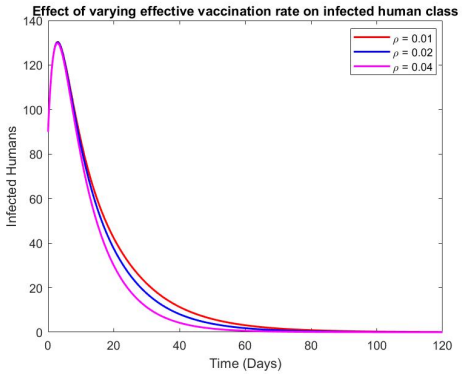

FIGURE 6. Infected Humans

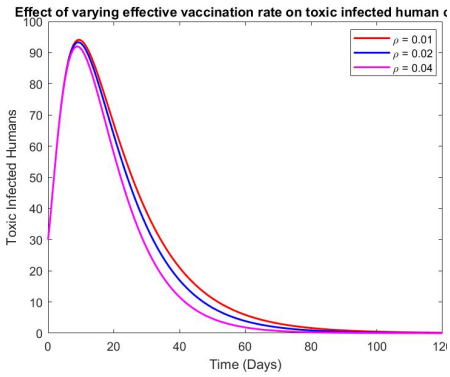

FIGURE 7. Toxic Humans

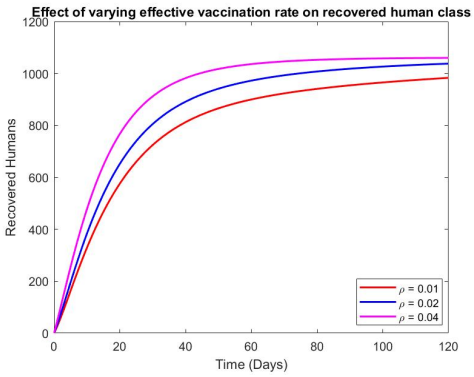

FIGURE 8. Recovered Humans

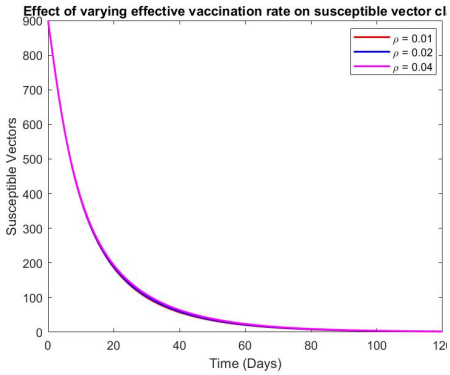

FIGURE 9. Susceptible Vectors

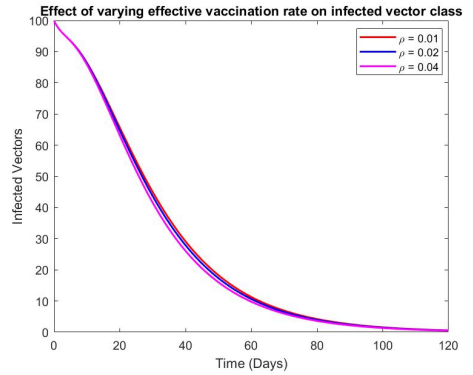

FIGURE 10. Infected Vectors

5. CONCLUSION

In this paper, a mathematical analysis of an epidemiological model for the infection dynamics and control of yellow fever epidemics with toxic infections is presented. The model disease-free state is determined and the conditions for the existence of a unique disease persistent state is also established. Additionally, with the help of the model disease reproductive number, we provided the conditions for the asymptotic stability of these equilibria. Furthermore, local sensitivity was conducted on the model parameters and it was ascertained that yellow fever epidemic is mostly influenced by the disease vectors average biting rate and the removal rate of these vectors from the population. Finally, numerical simulations were performed to support our stability

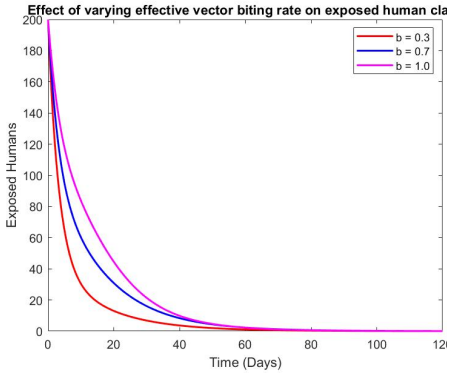

FIGURE 11. Exposed Humans

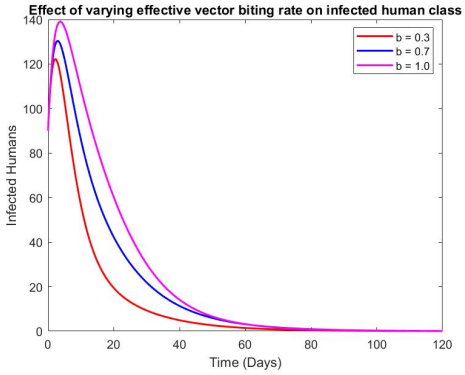

FIGURE 12. Infected Humans

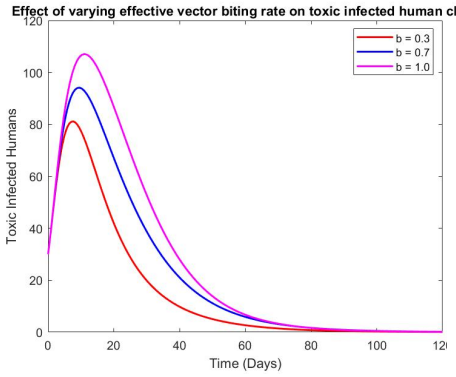

FIGURE 13. Toxic Humans

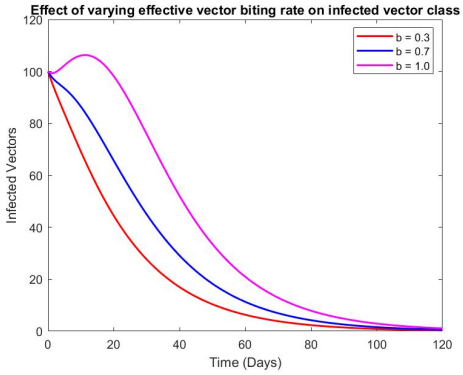

FIGURE 14. Infected Humans

analysis. The simulation results suggested that a high effective vaccination rate has the potential to minimize the yellow fever susceptibility rate.

ACKNOWLEDGMENT

The author sincerely appreciates the diverse support from colleagues towards the preparation of this manuscript. Much appreciation also goes to the reviewers for their constructive comments and guidance.

DATA AVAILABILITY

In this manuscript, the data used to support the numerical analysis is from published yellow fever works.

CONFLICT OF INTERESTS

The author declares that there is no conflict of interests.

REFERENCES

[1] K.A.M. Gaythorpe, A. Hamlet, K. Jean, D. Garkauskas Ramos, L. Cibrelus, T. Garske, N. Ferguson, The global burden of yellow fever, Elife 10 (2021), e64670.

[2] B.D. Handari, D. Aldila, B.O. Dewi, H. Rosuliyana, S. Khosnaw, Analysis of yellow fever prevention strategy from the perspective of mathematical model and cost-effectiveness analysis, Math. Biosci. Eng. 19 (2022), 1786–1824.

[3] N.P. Lindsey, J. Horton, A.D.T. Barrett, M. Demanou, T.P. Monath, O. Tomori, M. Van Herp, H. Zeller, I.S. Fall, L. Cibrelus, et al., Yellow fever resurgence: An avoidable crisis?, npj Vaccines 7 (2022), 137.

[4] A.A. Grobbelaar, J. Weyer, N. Moolla, P.J. van Vuren, F. Moises, J.T. Paweska, Resurgence of yellow fever in angola, 2015–2016, Emerg. Infect. Dis. 22 (2016), 1854.

[5] S. Zhao, L. Stone, D. Gao, D. He, Modelling the large-scale yellow fever outbreak in luanda, angola, and the impact of vaccination, PLoS Negl. Trop. Dis. 12 (2018), e0006158.

[6] M.U.G. Kraemer, N.R. Faria, R.C. Reiner, N. Golding, B. Nikolay, S. Stasse, M.A. Johansson, H. Salje, O. Faye, G.R.W. Wint, et al., Spread of yellow fever virus outbreak in angola and the democratic republic of the congo 2015–16: a modelling study, Lancet Infect. Dis. 17 (2017), 330–338.

[7] J.-P. Chippaux, A. Chippaux, Yellow fever in africa and the americas: a historical and epidemiological perspective, J. Venom. Anim. Toxins Incl. Trop. Dis. 24 (2018), 20.

[8] T. Garske, M.D. Van Kerkhove, S. Yactayo, O. Ronveaux, R.F. Lewis, J.E. Staples, W. Perea, N.M. Ferguson, Yellow fever expert committee, Yellow fever in africa: estimating the burden of disease and impact of mass vaccination from outbreak and serological data, PLoS Med. 11 (2014), e1001638.

[9] K. Jean, A. Hamlet, J. Benzler, L. Cibrelus, K.A.M. Gaythorpe, A. Sall, N.M. Ferguson, T. Garske, Eliminating yellow fever epidemics in africa: Vaccine demand forecast and impact modelling, PLoS Negl. Trop. Dis. 14 (2020), e0008304.

[10] T.T. Yusuf, D.O. Daniel, Mathematical modeling of yellow fever transmission dynamics with multiple control measures, Asian Res. J. Math. (2019), 1–15.

[11] M. Konlan, B.A. Danquah, A. Iddrisu, Mathematical modelling to assess the impact of a hypothetical vaccine on the dynamics of human onchocerciasis, Commun. Math. Biol. Neurosci. (2025), Article ID.

[12] R. Msuya, S. Mirau, N. Nyerere, I. Mbalawata, Modeling the impact of short-term displacement of domestic animals on the transmission dynamics of brucellosis, Heliyon 10 (2024).

[13] M. Konlan, B.A. Danquah, E. Okyere, S. Osman, J.A. Kessie, E.K. Donkoh, Global stability analysis and modelling onchocerciasis transmission dynamics with control measures, Infect. Ecol. Epidemiol. 14 (2024), 2347941.

[14] U.A. Danbaba, S.M. Garba, Stability analysis and optimal control for yellow fever model with vertical transmission, Int. J. Appl. Comput. Math. 6 (2020), 105.

[15] P. Kalra, I. Ratti, Mathematical modeling on yellow fever with effect of awareness through media, J. Phys. Conf. Ser. 2267 (2022), 012034.

[16] K. Fraser, A. Hamlet, K. Jean, D. Garkauskas Ramos, A. Romano, J. Horton, L. Cibrelus, N.M. Ferguson, K.A.M. Gaythorpe, Assessing yellow fever outbreak potential and implications for vaccine strategy, PLOS Glob. Public Health 4 (2024), e0003781.

[17] S. Zhao, S.S. Musa, J.T. Hebert, P. Cao, J. Ran, J. Meng, D. He, J. Qin, Modelling the effective reproduction number of vector-borne diseases: the yellow fever outbreak in luanda, angola 2015–2016 as an example, PeerJ 8 (2020), e8601.

[18] S.M. Raimundo, M. Amaku, E. Massad, Equilibrium analysis of a yellow fever dynamical model with vaccination, Comput. Math. Methods Med. (2015), 482091.

[19] P. Van den Driessche, J. Watmough, Reproduction numbers and sub-threshold endemic equilibria for compartmental models of disease transmission, Math. Biosci. 180 (2002), 29–48.

[20] M. Konlan, R.G. Chuaya, Stability analysis of a mathematical model for examination malpractice dynamics, Eur. J. Math. Anal. 5 (2025), 16–16.

[21] M. Konlan, R.I.M. Gunu, A.-K. Iddrisu, Mathematical modelling and analysis of measles control using vaccination, OALib 13 (2026), 1–18.

[22] M. Konlan, Modeling the inflow of exposed and infected migrants on the dynamics of malaria, Eur. J. Math. Anal. 4 (2024), 7–7.

[23] Y. Dumont, F. Chiroleu, C. Domerg, On a temporal model for the chikungunya disease: modeling, theory and numerics, Math. Biosci. 213 (2008), 80–91.

[24] J.C. Kamgang, G. Sallet, Global asymptotic stability for the disease free equilibrium for epidemiological models, C. R. Math. 341 (2005), 433–438.

[25] R.G. Chuaya, M. Konlan, Analysis of a mathematical model of corruption as an epidemic, OALib 12 (2025), 1–18.

[26] N.K. Goswami, S. Olaniyi, S.F. Abimbade, F.M. Chuma, A mathematical model for investigating the effect of media awareness programs on the spread of covid-19 with optimal control, Healthcare Anal. 5 (2024), 100300.